JOURNAL OF MATERIALS SCIENCE 3 (1968) 229-238

Mixed Oxides Prepared with an Induction Plasma Torch

Part 1 *Chromia/Alumina*

T. I. BARRY, R. K. BAYLISS, L. A. LAY
Inorganic and Metallic Structure Division, National Physical Laboratory, Teddington, Middx, UK

Received 6 November 1967, and in revised form 21 December

Pure and mixed aluminium and chromium oxides have been prepared by passage of the halides through a radio-frequency oxidising plasma. The nature of the materials produced has been assessed by electron microscopy, electron diffraction, X-ray diffraction, magnetic susceptibility, and electron spin resonance. The products were finely divided solids, containing mostly spherical particles in the size range 0.01 to 0.15 μm; however, the chromia particles were often hexagonal platelets up to 0.4 μm in diameter. The X-ray diffraction patterns were well defined, showing δ-alumina and α-chromia as major phases, and θ-alumina as a minor phase. The maximum degree of solid solution of chromium ions in the δ-alumina was limited to about 6% of the total cation content; solid solution of aluminium ions in the α-chromia phase was below the detection limit of 10%.

The nature of the particles, the phases produced, and the degree of solid solution are shown to be consistent with a sequence of condensation which can be predicted from thermodynamic data.

1. Introduction

High surface area mixed metal oxides are much used as catalysts, pigments, fillers, etc. For such materials it is often necessary to enhance or minimise chemical activity by controlled dispersion of additive metal oxides, maximum effectiveness being achieved when the additive oxide is dispersed as finely as possible in a controlled valence state on the surface of the support. The normal method of preparation of mixed oxides is by co-precipitation of decomposable compounds followed by a heat treatment which commonly leads to deleterious aggregation of the dispersed oxide and loss of surface area by sintering; contamination with bound hydroxyl ions is particularly difficult to avoid.

Finely divided metal oxides may be produced with the aid of a plasma torch, in a way which not only avoids some of the usual problems of contamination and sintering, but which also offers positive advantages in the possibility of control of atmosphere during preparation. The present work sets out to examine the characteristics of oxides prepared in this way, and to consider these characteristics in relation to the condensation process. The chromia/alumina system is particularly appropriate for such a study because it has been used as a model catalyst [1] system, and because alumina has previously been prepared by flame [2-5] and DC plasma [6] techniques. Because of the very small particle size and composite nature of the products, it is necessary to apply a range of techniques in their characterisation. Accordingly, the results are described in some detail so that the weight to be given to the observations from each technique can be assessed.

2. Experimental

2.1. Materials

Reagent grade CrO_2Cl_2 and $AlCl_3$ were used. They were redistilled where necessary.

2.2. Apparatus

The radio-frequency plasma torch was energised by a Radyne C240P 25 kW unit which operated at 5.8 Mc/sec. The normal anode power level was set at 4.5 kV and 3.75 A. The torch design is shown in fig. 1. The plasma was generated in the argon-rich central zone, and was stabilised by a fast annular flow of oxygen which was also necessary for conversion of halides to oxides. The metal halides were evaporated into supplementary argon streams and were mixed just prior to entering the central feed tube.

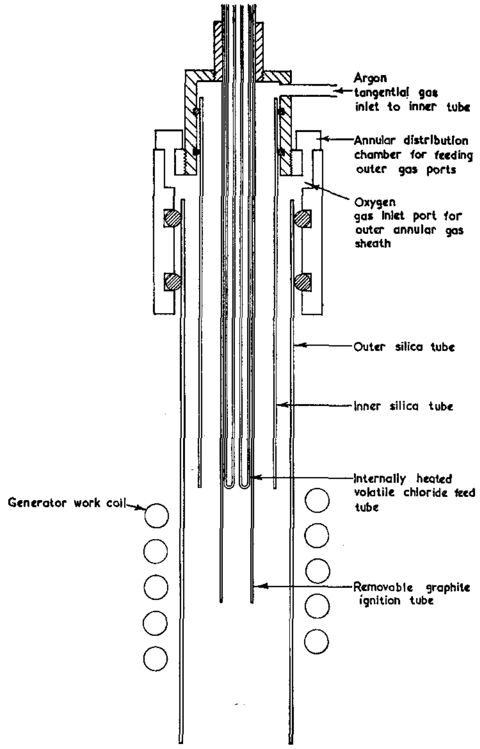

Figure 1 The RF plasma torch. The graphite ignition tube is withdrawn once the plasma is running.

The gas and entrained products from the tail flame were passed into a Pyrex tube of diameter 7.5 cm and then drawn by an exhaust system into aluminium ducting containing an electrostatic precipitator. The products described in this paper came from the Pyrex tube. The total recovery ratio of oxides from halides was 50 to 60%. Table I gives a list of experimental information. Further work in the National Physical Laboratory has much improved the efficiency of the torch.

TABLE I Operating conditions.

Inner argon flow rate = 11 l/min (300° K)
Outer oxygen flow rate = 42 l/min (300° K)
Cross sectional area of collection tube = 45 cm^2
Gas velocity at 2000° K = 130 cm/sec
Approximate longitudinal temperature gradient at 2000° K = 50° C/cm
Rate of production of solid = 2.8 × 10^{-4} g/sec
Mass of Al_2O_3 produced per unit volume of gas at 2000° K = 5 × 10^{-8} g/cm^3

2.3. Chemical and Spectrographic Analysis

The products from the torch were analysed chemically for chromium and aluminium. Chloride occurred to a variable extent; from less than 0.1 to 1.5 wt % was detected. Impurities detected by emission spectrography were $SiO_2 <$ 1 wt %; Mg, Ti and Sn < 0.1 wt %. These impurities may have been drawn in as dust in the atmosphere by the exhaust system.

2.4. Electron Microscopy

Observations were made with a JEM-7 electron microscope. Direct electron transmission photographs were taken of specimens which had been dispersed on to a carbon film supported on a grid. In some cases it was possible to take electron diffraction photographs of single particles.

2.5. Magnetic Susceptibility Measurements

Magnetic susceptibility measurements were made in a helium atmosphere by the Faraday method. Measurements were made over the temperature range −195 to +600° C. Specimens could be treated with any desired gas *in situ*. In order to avoid "glowing" the specimens due to exothermic reactions, the temperature was slowly raised to 600° C in the presence of the required gas at 5° C/min.

2.6. Electron Spin Resonance

Observations of esr were made on specimens in evacuated silica tubes by means of a Decca spectrometer which used a fixed frequency of 9270 Mc/sec. Most measurements were made at approximately 25° C, but some specimens were examined over a range of temperatures.

3. Results

3.1. Physical Characteristics

The products were fine, light, powders, which could be made into pellets without the use of a binder. The colours and compositions of the specimens are given in table II, together with the X-ray data. The specimens are identified by numbers which approximately define their cation compositions. Reduction in hydrogen at 600° C changed the colour of specimens containing appreciable concentrations of chromium to bright green. This is the colour of stoichiometric Cr_2O_3; thus the duller or darker colours of unreduced specimens were probably due to oxygen excess non-stoichiometry.

3.2. Electron Microscopy

Electron micrographs showed that for specimens containing up to 7.4% Cr, the particles were spherical, and in the size range 0.01 to 0.15 μm. Fig. 2a is representative for these specimens. Diffraction contrast observable in some of the spheres revealed that although they were not single crystals, many contained comparatively large single-crystal regions. In some instances steps could be seen on the edge of spheres at their intersection with zones of diffraction contrast. For 23% Cr/77% Al some of the particles were non-spherical with no particular shape dominating. For 100% Cr, some particles were thin hexagonal platelets with diameters up to 0.4 μm as shown in fig. 2b. These were probably α-chromia.

3.3. X-ray Diffraction

Because the particle size range is from 0.01 to 0.15 μm, and because sharp lines can be expected only for crystals greater than 0.03 μm in cross section, the X-ray diffraction photographs do not necessarily give a complete representation of the crystal phases present. The X-ray diffraction pattern of 100% Al contained no sharp reflections other than those assigned by Rooksby [7] to δ- and θ-aluminas. The pattern of δ-alumina was well developed, but θ-alumina was identified only by very faint reflections at $d = 4.53$ Å and 2.43 Å, the other diagnostic reflections described by Rooksby being absent. The presence of amorphous or glassy alumina was indicated by a broad halo centred at 4.6 Å.

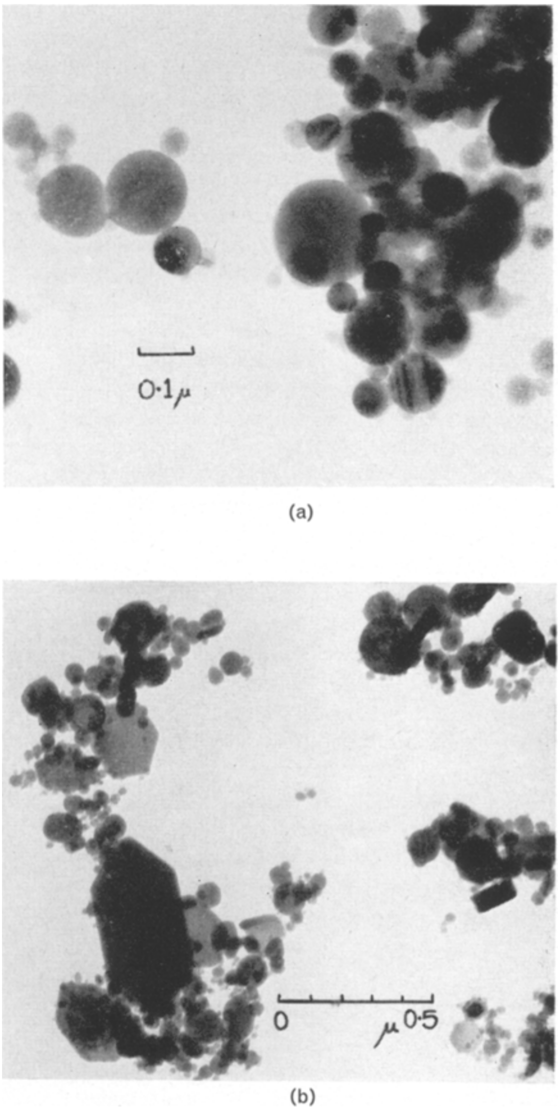

(a)

(b)

Figure 2 (a) Electron micrograph of 0.6% Cr/99.4% Al. (b) Electron micrograph of 100% Cr.

The presence of chromium-ions left the main features of the diffraction pattern unchanged, but a number of minor changes could be observed as follows. The halo, due to amorphous alumina, was weakened by even small additions of chromium. The δ-alumina pattern was appreciably sharper for specimens containing 0.3 to 1.0 at. % Cr than for pure alumina, but at higher concentrations of chromium the sharpness of the reflections was lost. The d-spacings of the δ-alumina lattice increased slightly with increasing chromium content; the calculated unit cell dimensions are given in table II together with other details. However, since no special precautions were taken in the preparation of the specimen or the film, the values should be taken only as indicating a trend. The addition of chromium also has the effect of increasing the proportion of θ-alumina. For all specimens containing between 0.37 and 4.7 at. % Cr, the reflection at 4.53 Å became equal in intensity to the nearby reflections of δ-alumina at approximately 5.07 Å and 4.05 Å. In 5% Cr/95% Al an additional reflection of θ-alumina occurred at 2.86 Å, but other reflections of this phase were still absent. A weak unidentified reflection was found at 2.36 Å.

The α-chromia diffraction pattern, detected first by a single reflection for 7% Cr/93% Al, became well developed in 23% Cr/77% Al, the strongest reflections being equal in intensity to those of δ-alumina. The *d*-spacings of the α-chromia pattern did not depart significantly from the values given in the ASTM index for pure α-chromia. The error in this estimation would not exceed 0.1%. With this limit of error it would certainly be possible to detect the solid solution of 10% alumina in the α-chromia lattice [8], and these observations reveal the striking result that even though the concentration of $AlCl_3$ in the feed to the plasma exceeded that of CrO_2Cl_2, solid solution of alumina in the α-chromia lattice was insignificant. For 23% Cr/77% Al the intensities of the reflections due to α-chromia also agreed reasonably well with the ASTM index. This result contrasts with that for 100% Cr for which the hk0 reflections, 110, 300, and 220, were relatively augmented. The most probable reason for the weakness of the other reflections lies in the platelike character of the hexagonal α-chromia particles, which because of their size have a disproportionate effect on the X-ray pattern. These facts, taken together with the evidence from electron micrography, show that the alumina has an effect on the morphology of chromia in that it restricts the formation of hexagonal platelets.

An estimate of the fraction of the chromium present as particles of α-Cr_2O_3 can be obtained by a comparison of the intensities of X-ray reflections from the specimens with those from synthetic mixtures of α-Cr_2O_3 and alumina from the plasma as shown in fig. 3. High purity α-Cr_2O_3 from Koch-Light Ltd* was used together with 0.4% Cr/99.6% Al in the synthetic mixtures. (100% Al was not used because it gave less sharp reflections than 0.4% Cr/99.6% Al, and 100% Cr was unsuitable because it gave abnormal intensities.) Fig. 3 illustrates the correspondence between the intensities for 7% Cr/93% Al and the mixture containing 1 wt % Cr_2O_3, and for 23% Cr/77% Al and the mixture containing 20 wt % Cr_2O_3. From these values the calculated fractions of chromium appearing as Cr_2O_3 are 0.10 in 7% Cr/93% Al, and 0.64 in 23% Cr/77% Al. If it is assumed that the aluminium content of the Cr_2O_3 phase is insignificant, then the residual chromium expressed as a fraction of total cations in the alumina phase is 0.067 for 7% Cr/93% Al, and 0.099 for 23% Cr/77% Al. However, if, as seems possible, the X-ray reflections from the pure Cr_2O_3 phase in the synthetic mixtures are more intense than those from the same weight fraction of Cr_2O_3 particles in the specimens, then the calculations of this fraction must be adjusted.

Specimens used for magnetic susceptibility measurements and subjected to an oxidation, reduction cycle showed no significant change in

TABLE II

Sample no	Cr at. % of total cations	Colour	X-ray		
			phases found*	δ unit cell	θ lines
100% Al	0.00	white	δ; θ amorph.	$a = 7.96$ $c = 11.73$	4.55 2.43
0.4% Cr/99.6% Al	0.37	white	δ, θ	$a = 7.96$ $c = 11.74$	4.55 2.43
0.6% Cr/99.4% Al	0.65	off white	δ, θ	$a = 7.96$ $c = 11.74$	4.55 2.86 2.43
5% Cr/95% Al	4.60	grey	δ, θ	$a = 8.01$ $c = 11.79$	4.55 2.86 2.43
7% Cr/93% Al	7.40	grey	δ, θ α	$a = 7.99$ $c = 11.80$	4.55 2.43
23% Cr/77% Al	23.30	grey green	δ, α	$a \sim 8.00$ $c \simeq 11.8$	

*δ and θ indicate δ- and θ-aluminas respectively, and α indicates α-chromia.

---

*Address: Colnbrook, Bucks, UK

X-ray diffractions pattern from untreated specimens.

3.4. Electron Spin Resonance

Three basic types of spectra were found for chromium-ions in the specimens. These arose from (i) Cr^{5+}-ions, (ii) individual Cr^{3+}-ions, and (iii) clusters of Cr^{3+} including material of composition close to Cr_2O_3. Fig. 4 shows the spectra from 7% Cr/93% Al obtained over the temperature range 113 to 473° K. The components of the spectra are identified in fig. 4 and are discussed in sequence below.

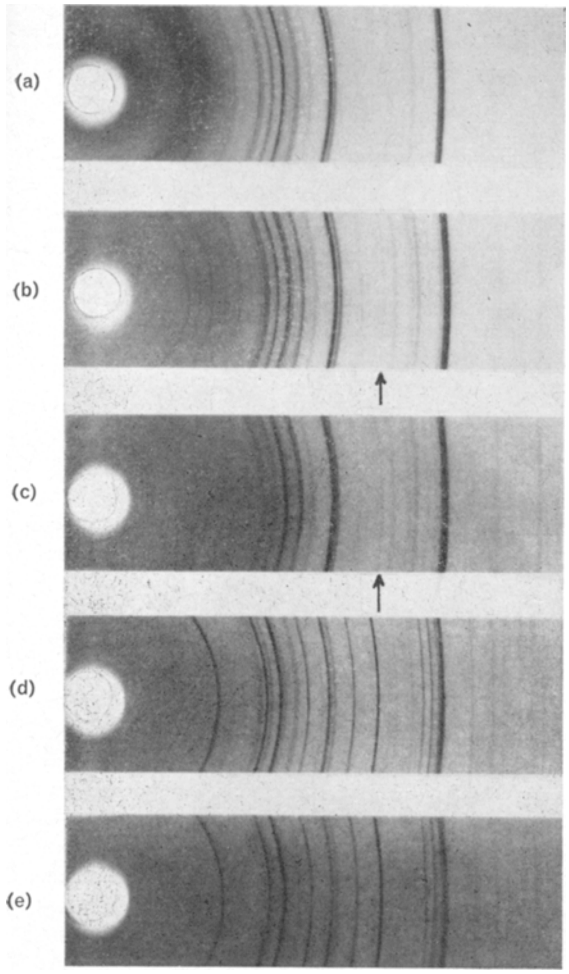

Figure 3 X-ray diffraction patterns of chromia/alumina specimens compared with synthetic mixtures. (a) 100% Al; (b) chromia/alumina mixture containing 1 wt% Cr_2O_3; (c) 7% Cr/93% Al; (d) chromia/alumina mixture containing 20 wt% Cr_2O_3; (e) 23% Cr/77% Al. CuK_α radiation. The arrows point to the reflection from α-chromia with *d*-spacing 1.68 Å.

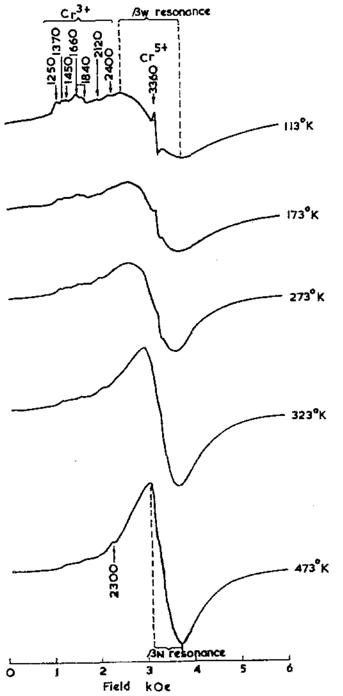

Figure 4 Esr spectra of 7% Cr/93% Al measured at 9270 Mc/sec.

TABLE III Susceptibility data for chromia/alumina specimens.

Sample, and gas treatment	Fractional wt Cr_2O_3	f	g	$1-f-g$	θ° K	Cr^{3+} cation fraction of alumina phase	$m \times 10^6$ wt fraction of iron
0.6% Cr/99.4% Al H_2	0.0095	1.00	0.00	0	0	0.0065	0.4
5% Cr/95% Al O_2	0.067	0.42	0.50	0.08	−20	0.021	1.5
5% Cr/95% Al H_2	0.067	0.44	0.56	0	0	0.022	8.1
23% Cr/77% Al O_2	0.312	0.115	0.80	0.085	0	0.035	0.0
23% Cr/77% Al H_2	0.312	0.125	0.875	0	−60	0.038	2.8

(i) The spectrum due to Cr^{5+} at 3360 Oe has $g = 1.968$, and line width = 55 Oe. It is thus identical to that found by other workers [9-12]. The spectrum is strongest when the Cr concentration is below 1 at. %. Cr^{5+} is more sensitively detected than Cr^{3+}, so that the actual concentration is not high.

(ii) The weak but well defined peaks from 1250 to 1840 Oe are all due to isolated Cr^{3+}-ions. (No peaks due to Fe^{3+} or other impurities were found in this region of the spectrum in the specimen containing no chromium.) Within the large limits of experimental error, the intensities of the resonances due to individual Cr^{3+}-ions were independent of the chromium content of the specimens when this exceeded 0.6 %. Moreover, there was no change in line width with increasing Cr concentration. These observations indicate that solution of Cr^{3+}-ions in the alumina was very restricted. The spectra from individual Cr^{3+}-ions are discussed more fully in the appendix.

(iii) The β_W resonance ascribed by Poole *et al* [13-15] to weakly coupled clusters is characterised in the present work by a broad resonance extending over about 1100 Oe and centred at about 3000 Oe. It can be observed best either in specimens containing low concentrations of chromium at room temperature, or in specimens containing higher concentrations of chromium at about 150° K. The fact that the intensity of the β_W resonance does not decrease with decreasing temperature between 173 and 113° K indicates that the magnetic coupling is weak. Approximate measurements of the β_W resonance show that it has an intensity independent of chromium concentration when this exceeds 5 at. %. In the present work it seems probable that the β_W resonance arises from clusters of Cr^{3+}-ions on the surface of alumina particles.

The β_N resonance which occurs in specimens containing >4 at. % has a line width of 600 Oe at temperatures above 400° K. The sharp loss of the resonance between 320 and 273° K, i.e. below the Néel point of α-Cr_2O_3, confirms the conclusion of Poole and Itzel [14] that material of composition and structure close to α-Cr_2O_3 is responsible for the β_W resonance. This result is supported by X-ray data which show that the α-Cr_2O_3 present in 23 % Cr/77 % Al contained less than 10 at. % alumina.

In addition to the spectral features already discussed, there is a small peak which changes in field with changing temperature. At 473° K it occurs at 2300 Oe, whereas at 113° K it has moved to 2120 Oe. Moreover, the intensity of the peak increases slightly, but steadily, with increasing temperature. Probably it arises from some specific exchange-coupled pair of Cr^{3+}-ions.

3.5. Magnetic Susceptibility Measurements

The aim of the magnetic susceptibility measurements is to determine the proportion of Cr^{3+}-ions in solid solution in the alumina. In order to eliminate effects due to ferromagnetism, the susceptibility χ was determined by use of the equation

$$\frac{p}{W} = \frac{mI}{\rho}\frac{dH}{dx} + (\chi + \chi_c)\, H \frac{dH}{dx} \qquad (1)$$

where p is the force on the specimen of mass W, which contains a small ferromagnetic component of fractional mass m, density ρ, and magnetisation intensity I. The specimen was suspended in a magnetic field H, and vertical field gradient dH/dx. χ_c is the diamagnetic susceptibility of the cores of the atoms. A plot of p/W divided by dH/dx against H gives the slope $(\chi + \chi_c)$ and intercept mI/ρ. In reduced specimens, a marked fall in mI/ρ occurring between 770 and 870° K was probably due to small particles of iron. The fractional weights of iron necessary to account for the observed effects are recorded in table III, column 8. Very small particles of iron might be expected to be superparamagnetic, i.e. to have a high, field-dependent susceptibility in the temperature range from 400 to 900° K, which probably accounts for the anomalous behaviour of 5 % Cr/95 % Al in this temperature range.

The experimentally determined values of susceptibility derived from equation 1 are compared in fig. 5, with curves derived from the equation

$$\chi/y = f\chi_D + g\chi_N \qquad (2)$$

where y is total chromium content per gram of specimen expressed as Cr_2O_3, f is the fraction of the chromium in the form of dispersed Cr^{3+}-ions, and g is the fraction which behaves magnetically like Cr_2O_3. For reduced specimens, it is assumed that $(f + g) = 1$. χ_D and χ_N are the susceptibilities of the dispersed and non-dispersed Cr^{3+}-ions; they are given by the expressions

$$\chi_D = 0.0247/(T - \theta) \qquad (3)$$

where T is the absolute temperature, and θ is the Weiss constant, and

$$\chi_N = (17.5 + 0.025\,T) \times 10^{-6} \quad \text{between 80 and 300° K} \qquad (4)$$

This is an approximate relation derived from the data of Honda and Sone [16], and McGuire *et al* [17],

$$\chi_N = 0.0231/(T + 420) \text{ above 450° K} \qquad (5)$$

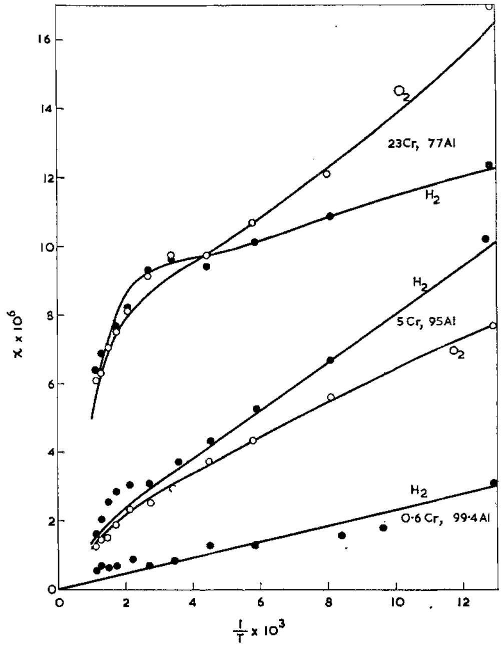

Figure 5 Magnetic susceptibilities of chromia/alumina specimens. ○, specimens pre-treated in O_2; ●, specimens pre-treated in H_2.

The value of $\theta = -420°$ K was chosen from the data of Bhatnagar *et al* [18] as appropriate for specimens of small particle size. The values of f and g are given in table III, together with the values of θ necessary to fit the data to equations 2 and 5. The X-ray studies show that the chromia/alumina specimens are heterogeneous mixtures of α-chromia and δ- and θ-aluminas containing some chromium-ions in solid solution. Calculations from equations 2 to 5 enable minimum values to be placed on the extent of this solid solution. For this purpose it is necessary to assume that all the Cr^{3+}-ions in the Cr_2O_3 particles behave magnetically like those in bulk Cr_2O_3. With this assumption the minimum value of the fraction of Cr^{3+} in solid solution in alumina is given in table III, column 3, by f, which is converted in column 7 to the fraction of cation sites in the alumina phase which are occupied by chromium.

The calculated fractions of total Cr^{3+}, i.e. $(f + g)$, were less than 1 for specimens not treated in hydrogen. This denotes the presence of hexavalent chromium which is diamagnetic, and pentavalent chromium which has a low magnetic moment. The diamagnetic fraction of chromium is listed in table III, column 5. During reduction by hydrogen, aggregation of chromium-ions occurred, as shown by the increase in g. A complete cycle of oxidation, reduction and re-oxidation caused a permanent fall in the low temperature susceptibility of 5% Cr/95% Al. The susceptibility at 78° K, originally 7.30×10^{-6}, increased to 7.66×10^{-6} with oxidation, and to 10.21×10^{-6} with reduction, but fell to 7.09×10^{-6} upon re-oxidation. This irreversible fall is due to sintering of the Cr_2O_3 particles.

4. Discussion

4.1. The Degree of Solid Solution of Cr^{3+} in the Mixed Oxides

The methods of evaluation all indicate that the extent of solid solution is not a very sensitive function of chromium concentration at high chromium contents. Thus the maximum possible value of the atom fraction of Cr^{3+} present as individual ions or as small clusters in the alumina phases can be gauged from the results for 23% Cr/77% Al. The values from the three methods are: X-ray diffraction, 0.1; esr, ~0.05; magnetic susceptibility, 0.04. The discrepancies may be accounted for in two ways. First, X-ray diffraction underestimates the proportion of Cr_2O_3 present, and therefore overestimates the proportion of dispersed Cr^{3+}. Second, pairs of Cr^{3+}-ions in neighbouring sites in the alumina structure would have a very low temperature coefficient of magnetic susceptibility at temperatures below 300° K. Consequently these pairs would not be included in the fraction of dispersed Cr^{3+}-ions calculated from susceptibility data. Thus the most probable value for the maximum atom fraction of Cr^{3+} present as individual ions or as small clusters in the alumina phase is 0.05 to 0.07. Esr indicates that the fraction of well-separated Cr^{3+}-ions is only 0.01.

The discussion of the condensation process which follows aims to account for this low degree of solid solution, and also for the other features of the product, such as particle morphology and crystallography, which are summarised in the abstract.

4.2. Condensation Processes

During the conversion of metal chlorides to finely divided mixed metal oxides, the material passes rapidly through a wide temperature range. Thermodynamic data are unreliable for temperatures above 2000° K. Nevertheless, consideration of the data leads to a qualitative understanding of the condensation process which is in agreement with features of the observed product. Values from the JANAF tables [19] were used. As a basis for the following discussion it will be assumed that the gas phase reactions are rapid, and approach equilibrium, whereas processes in the condensed phases may lag behind equilibrium. The results are shown to be consistent with these assumptions.

4.3. Condensation of Alumina

The free energies of formation of gaseous aluminium chloride and oxide species are roughly comparable at the plasma temperature. However, oxide species will be produced predominantly, because of the large excess of oxygen in the plasma. A mass spectrometric examination of the vaporisation of alumina has been reported by Drowart *et al* [20] who observed the presence of Al, Al_2O, AlO, Al_2O_2, and O in the gas phase under neutral conditions. As pointed out by Alcock [21], the dissociative vaporisation of oxides must be suppressed by oxygen. Calculations show that in one atmosphere oxygen pressure the vapour pressures of Al, Al_2O, AlO, and Al_2O_2 are negligibly small even at 3000° K, compared with the partial pressure of alumina feed material in the plasma. Thus condensation of alumina to liquid droplets may commence at temperatures as high as 3000° K, and is likely to be complete before crystallisation of alumina occurs at 2320° K or lower, because the supersaturation in the gas phase would be very high at this temperature.

The melting point of δ-alumina is necessarily lower than that of the stable phase α-alumina. Possible reasons for the occurrence of the δ- rather than the α-form in flame-sprayed particles are discussed by Plummer [2] and Rooksby [22]. Plummer considers that in the liquid phase a large proportion of aluminium atoms have tetrahedral rather than octahedral co-ordination. He gives arguments to show that, with rapid quenching, the existence of tetrahedrally co-ordinated aluminium atoms will lead to the formation of a cubic, close-packed oxygen lattice, whereas, under equilibrium conditions, all the aluminium atoms have time to move into octahedral sites, and this in turn leads to hexagonal packing of the oxygen atoms in the α-alumina structure.

The later work of Das and Fulrath [6] makes it clear that the phases of alumina found are determined primarily by the rates of nucleation rather than of crystallisation, the crystallisation rates being very rapid. This is confirmed by some recent work [23], in which we have found that only α-alumina was produced by quenching 50 μg specimens of liquid alumina in thermocouple loops [24, 25] at 10^4 ° C/sec. This is a somewhat faster rate of cooling than that achieved in the plasma torch. (Temperature gradients within the specimen can be shown to be negligible.) Presumably, the relatively large specimens, which are about 10^{12} times bigger than the particles from the plasma, have a high statistical probability of producing α-alumina nuclei during cooling. The undercooling of the alumina liquid was approximately 60° C at a cooling rate of 200 to 1000° C/sec.

4.4. Condensation of Chromia

The formation of chromium oxide particles from CrO_2Cl_2 probably follows a similar course to that of alumina particles, but differs in the important respect that condensation occurs directly to solid, rather than to liquid, particles. The melting point of Cr_2O_3, 2600° K, is higher than that of alumina, and the vapour pressure at this temperature is also higher. The data of Grimley, Burns, and Inghram [26] for the temperature range 1839 to 2059° K show that Cr_2O_3 vaporises congruently: Cr atoms, CrO, CrO_2, CrO_3, O, and O_2 co-exist in the gas phase. An extrapolation of the data shows that the vapour pressure at the melting point is very much greater than the partial pressure of chromium-bearing species in the tail flame. For this reason Cr_2O_3 must condense as solid particles, probably in the temperature range 2100 to 1900° K. The electron micrographs of fig. 2 show that the majority of particles of chromia have angular shapes, many with some hexagonal character, whereas other specimens have a great majority of spherical particles. These results suggest that there may be a correlation between the shape of the particles and whether they form initially as liquids or solids.

4.5. The Condensation of Chromia/Alumina Preparations

The vapour pressure of alumina is so low in the presence of oxygen that condensation of alumina must occur well in advance of the condensation of chromia, even when allowances are made for the low accommodation coefficient of alumina [21], and the lowering of the vapour pressure of chromia by solution in the alumina. Thus there can be no "co-precipitation" of the two oxides from the plasma, and solid solution of alumina in the chromia particles cannot occur. On the other hand, solution of chromia in the alumina could occur by a different process; chromium-ions might condense on the surface of liquid alumina droplets, and dissolve into the bulk. However, the experimental result of a low degree of solution of chromia in alumina shows that this process does occur, but to a limited extent.

The effect the chromium has in decreasing the proportion of amorphous alumina and increasing the proportion of θ-alumina implies that these chromium-ions condense on the alumina droplets before crystallisation occurs. The role of the chromium-ions in preventing the occurrence of amorphous material may be related to the strong octahedral site preference of Cr^{3+}-ions, and to the effect of transition metal ions in promoting the controlled nucleation of crystallisation of glass.

There is no reason to believe that the lack of solid solution in the plasma preparation is due to a low solubility at equilibrium. α-Cr_2O_3 and α-alumina form a complete range of solid solutions, and Cr^{3+} is likely to be soluble in the octahedral sites of δ-alumina.

Conclusions

(i) The preparation of alumina in an induction plasma torch leads mainly to δ-Al_2O_3 with some θ-Al_2O_3; both are metastable phases. The particles probably condense as liquid droplets at temperatures close to 3000° K because of the low vapour pressure of alumina in an oxygen atmosphere.

(ii) The preparation of chromia gives α-Cr_2O_3 containing a proportion of thin hexagonal platelets. This is consistent with the view that Cr_2O_3 condenses as a solid, probably in the temperature range 2100 to 1900° K.

(iii) For the mixed oxide system, solid solution of alumina in α-Cr_2O_3 was not detected, and solid solution of chromia in δ-Al_2O_3 was limited to 5 to 6%. The low degree of solid solution is attributed to the disparity in vapour pressures of the two oxides.

(iv) Alumina affects the morphology of the α-Cr_2O_3, which suggests that part of the limited degree of solid solution observed could be due to condensation of chromia vapour on alumina droplets.

Acknowledgements

The authors gratefully acknowledge help from D. Clinton for observations with the electron microscope, Miss J. Spink for the X-ray diffraction photographs, and G. H. Smith for chemical analyses.

References

1. R. P. EISCHENS and P. W. SELWOOD, *J. Amer. Chem. Soc.* **69** (1947) 1590, 2698.
2. M. PLUMMER, *J. Appl. Chem.* **8** (1958) 35.
3. R. CAILLAT, J. P. CUER, J. ELSTON, F. JUILLET, R. POINTUD, M. PRETTRE, and S. TEICHNER, *Bull. Soc. Chim. France* (1959) 152.
4. J. P. CUER, J. ELSTON, and S. J. TEICHNER, *ibid* (1961) 81, 89, 94.
5. H. P. ROOKSBY and C. J. M. ROOYMANS, *Clay Minerals Bulletin* **4** (1961) 234.
6. A. R. DAS and R. M. FULRATH, Proc. 5th Intern. Conf. Reactivity of Solids (1964) (Elsevier, Amsterdam 1965) p. 31.
7. H. P. ROOKSBY, "X-ray Identification and Crystal Structures of Clay Minerals", edited by Brown, Taylor, and Francis (Mineralogical Society, London, 1961) Chapter 10, p. 354.
8. J. GRAHAM, *J. Phys. Chem. Solids* **17** (1960) 18.
9. P. COSEE and L. L. VAN REIJEN, Proc. 2nd. Intern. Cong. of Catalysis (Technip, Paris, 1960) p. 1679.
10. L. L. VAN REIJEN, W. M. H. SACHTLER, P. COSEE, and L. BROUWER, Proc. 3rd. Intern. Cong. of Catalysis (North Holland Publishing Co, Amsterdam, 1964) p. 829.
11. L. L. VAN REIJEN, thesis, Technological University, Eindhoven (1964).
12. D. E. O'REILLY and D. S. MACIVER, *J. Phys. Chem.* **66** (1962) 276.
13. C. P. POOLE, W. L. KEHL, and D. S. MACIVER, *J. Catalysis* **1** (1962) 407.
14. C. P. POOLE and J. F. ITZEL, *J. Chem. Phys.* **41** (1964) 287.
15. C. P. POOLE and D. S. MACIVER, *Adv. Catalysis* **17** (1967) 224.
16. K. HONDA and T. SONE, *Science Reports Tôhoku Univ.* **3** (1914) 223.
17. T. R. MCGUIRE, E. J. SCOTT, and F. H. GRANNIS, *Phys. Rev.* **102** (1956) 4.
18. S. S. BHATNAGAR, A. CAMERON, E. H. HARBARD, P. L. KAPUR, A. KING, and B. PRAKASH, *J. Chem. Soc.* (1939) 1433.

19. JANAF Thermochemical Tables, USAF Contract No. AF 33 (616)-6149 (1962).
20. J. DROWART, G. DEMARIA, R. P. BURNS, and M. G. INGHRAM, *J. Chem. Phys.* **32** (1960) 1366.
21. C. B. ALCOCK, *Trans. Brit. Ceram. Soc.* **60** (1961) 147; **61** (1962) 667.
22. H. P. ROOKSBY, *J. Appl. Chem.* **8** (1958) 44.
23. T. I. BARRY and C. LEWIS, unpublished.
24. R. A. MERCER and R. P. MILLER, *J. Sci. Instr.* **40** (1963) 352.
25. W. GUTT, *ibid*, **41** (1964) 393.
26. R. T. GRIMLEY, R. P. BURNS, and M. G. INGHRAM, *J. Chem. Phys.* **34** (1961) 664.
27. M. PETER and A. L. SCHAWLOW, *Bull. Amer. Phys. Soc.* **5** (1960) 158.

Appendix

Electron spin resonance of individual Cr^{3+} centres

The use of the methods developed by van Reijen [11] indicates that at least three different sites are needed for the isolated Cr^{3+}-ions to account for the observed spectra. All the sites are likely to be in distorted octahedra of oxygen-ions. The fact that all the peaks occur at low fields indicates that the axial field parameter, D, is comparable to, or larger than, the microwave energy. If this is assumed to be the case, then the observed resonance peaks may be assigned to various degrees of orthorhombic distortion, E/D. For axial symmetry $E/D = 0$, and for maximum orthorhombic distortion $E/D = 1/3$. The g-value of 1.98 was used throughout.

(i) The peak at 1250 Oe with a shoulder at 1200 Oe can be assigned to a Cr^{3+} centre with $E/D = 0.25$. This is in accordance with the observations of van Reijen [11] on a specimen containing predominantly θ-alumina. The value of E/D was shown to be consistent both with the structure of θ-Al_2O_3, and the data of Peter and Schawlow [27] on iso-structural β-Ga_2O_3. Another peak should occur at 2700 Oe, but this is likely to be weaker and broader than the peak at 1250 Oe.

(ii) The peaks at 1660 and 1840 Oe could arise from Cr^{3+} in a site of close to axial symmetry with only a slight orthorhombic distortion. $E/D = 0.05$.

(iii) The peaks at 1370 and 1450 Oe may be due to Cr^{3+} centres in two different sites, with values of E/D close to 0.15. The peak at 2400 Oe may also be due to one of these centres. However, these assignments are less definite than those discussed in paragraphs (i) and (ii).

The spectra described in paragraphs (ii) and (iii) almost certainly arise from individual Cr^{3+}-ions in δ-alumina, but neither unambiguously fits the data of van Reijen [11]. The field values found by van Reijen were 1360 and 1550 Oe (values adjusted to suit our microwave frequency). However, van Reijen's δ-alumina was prepared from Bohemite, and the X-ray pattern was poorly developed.